Microcontroller based closed-loop control of a 2D quasi-static/resonant microscanner with on-chip piezo-resistive sensor feedback

Richard Schroedter[a], Markus Schwarzenberg[a], André Dreyhaupt[a], Robert Barth[a], Thilo Sandner[a], and Klaus Janschek[b]

[a]Fraunhofer Institute for Photonic Microsystems (FhG-IPMS), AMS, Microscanner R&D, Dresden, Germany
[b]Institute of Automation, Faculty of Electrical and Computer Engineering, Technische Universität Dresden, 01062 Dresden, Germany

ABSTRACT

In this paper we present a 2D raster scanning quasi-static/resonant micro mirror being controlled in both axes in closed-loop with on-chip piezo-resistive sensor feedback. While the resonant axis oscillates with a given frequency, the quasi-static axis allows static as well as dynamic deflection up to its eigenfrequency because of its staggered vertical comb (SVC) drive arrangement. Due to the high quality factor of the very low damped spring-mass-system, an adapted trajectory planning using jerk limitation is applied for the quasi-static axis [1]. Nevertheless, inaccuracies of the applied nonlinear micro mirror model and external disturbances lead to undesired residual oscillation in open-loop control mode. To achieve high precise and fast beam positioning, we implement a flatness-based control algorithm with feedback to on-chip piezo-resistive deflection sensors. In comparison to previous work [2,3], we developed a micro controller setup for driving the microscanner, that is equipped with an analog Bessel filter increasing the sensor signal quality significantly. In this study we demonstrate a small size and low power micro mirror driver including high-voltage generation and a microcontroller for real-time control as well as a head circuit board for high resolution sensing. We discuss experimental results of open-loop and closed-loop control for 2D raster scanning operation. Finally, the outlook is given to the intrinsic capability to compensate temperature drifts influencing the piezo-resistive sensor signal.

Keywords: quasi-static, electrostatic, micro mirror, 2D raster scan, staggered vertical comb drive, piezo-resistive sensor, flatness-based closed loop control, microcontroller based mirror driver, residual oscillation

1. INTRODUCTION

Micro scanning mirrors (MSMs) enable dynamic deflection of collimated light (e.g. laser) about one (1D) or two (2D) scan axes needed for a broad field of applications. Numerous MSMs with different physical actuation principles (e.g. electrostatic, electromagnetic, piezoelectric, electro-thermal) device concepts and technologies have been realized so far [4]. Electrostatic MSMs, like the ones fabricated by Fraunhofer IPMS, are preferred for commercial applications because of their small size and allow for high-speed scanning at very low power consumption and high mechanical robustness against vibration and shock. In addition, MSMs utilized of single crystalline silicon (c-Si) show excellent long run behavior and low sensitivity to ambient temperature. These qualities make MSMs attractive for highly miniaturized and mobile applications. Early applications (using resonant MSM) were focused on scanning imaging systems such as e.g. bar code reading and confocal microscopy. Next, optical cross-connects for telecommunication fiber networks - requiring quasi-static 2D-MSMs - where the main driver for MEMS scanner technology around the turn of the new millennium. During the last decade miniaturized laser projection displays with its large demands on scan frequency, scanning angle, optical resolution and miniaturization became the technology driver for MSM. In our days MEMS scanners focus on various medical

Further author information: (Send correspondence to Richard Schroedter)
Richard Schroedter: E-mail: richard.schroedter@ipms.fraunhofer.de, Telephone: + 49 351 8823 196
Klaus Janschek: E-mail: klaus.janschek@tu-dresden.de, Telephone: +49 351 463 34025

Post-print version of the article: R. Schroedter, M. Schwarzenberg, A. Dreyhaupt, R. Barth, T. Sandner, K. Janschek, "Microcontroller based closed-loop control of a 2D quasi-static/resonant microscanner with on-chip piezo-resistive sensor feedback", *Proc. of SPIE, MOEMS and Miniaturized Systems XVI*, vol. 10116, p. 1011605, 2017. DOI: 10.1117/12.2251802

imaging applications, optical coherence tomography (OCT), tunable laser sources as well as light detection and ranging (LIDAR) systems for automotive industry (e.g. for autonomous car navigation).

Bi-resonant 2D-MSMs, e.g. the resonant 2D-MSM of IPMS with *in-plane* comb drives and proven for reliable industrial fabrication [5,6], are limited to resonant operation at fixed frequency or frequency ratio. Thus, the scan trajectory is fixed and depends on the amplitude and the frequency ratio predefined by the MEMS design. To enhance the optical resolution and/or frame rate of laser scanning projection and imaging systems a progressive raster scanning pattern with linear vertical (e.g. sawtooth) scan trajectory (see Fig. 1b) is preferred over a bi-resonant Lissajous figure scanning. Therefore, a quasi-static actuation of the vertical scan axis is required. For that reason, IPMS extended its scanner technology to quasi-static actuation using three-dimensional vertical *out-of-plane comb* drives. The IPMS device concept for vertical 3D comb drives - named *LinScan* - was realized as system-in-package device and assembly [7, 8]. The presented gimballed 2D quasi-static/resonant microscanner, Fig. 1a, can realize a raster scan by combining a sawtooth motion of the outer quasi-static axis (driven by staggered vertical comb (SVC) drives) and a resonant motion of the inner resonant axis. Even though the quasi-static axis can provide substantial static tilt up to ±7 degree due to its SVC comb drives, it still represents a high quality factor spring mass system which is very lowly damped by the surrounding viscous gas. To guarantee high precise linearized scan trajectories the quasi-static scan axis has to be controlled.

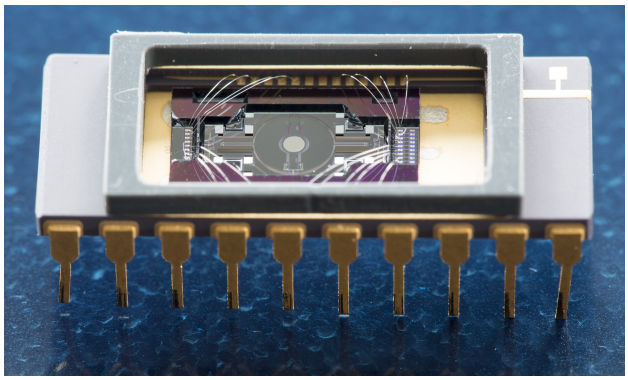

(a) Photograph of mounted scanner

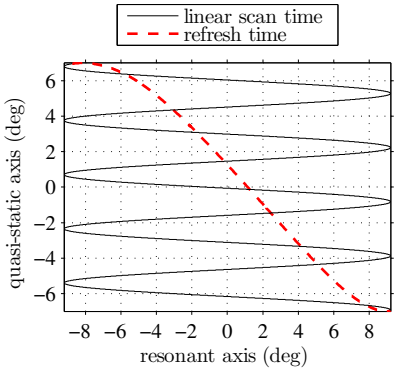

(b) 2D raster scan

Figure 1: (a) 2D quasi-static/resonant microscanner, (b) 2D raster scan (with 8.85 Hz sawtooth for quasi-static axis and 44.25 Hz sinus for resonant axis, reduced to 1/100 of applied frequency f_{res} for better visibility)

In previous works, we concentrated on open-loop control strategies [1] and real-time closed-loop control with optical feedback [2,3] applying a robust linear PID controller as well as flatness-based control as system inversion and sliding-mode control. Due to the very low damping, an adapted trajectory command shaping using jerk limitation was applied [1]. Nevertheless, inaccuracies of the applied nonlinear micro mirror model and external disturbances lead to undesired residual oscillation in open-loop control mode. To achieve high precise and fast beam positioning, we implement a flatness-based control algorithm with feedback from on-chip piezo-resistive deflection sensors. In comparison to the previous work [2, 3], we present in this paper a new micro controller setup for closed-loop driving of the quasi-static/resonant raster scanning mirror.

This paper is organized as follows: In section 2 we introduce the 2D quasi-static/resonant microscanner describing its functionality and identifying the parameter used for real-time control. We present the control algorithms for each axis in section 3. In section 4 the assembling and its key parameter of the microcontroller based driver are given. We evaluate the control results and the scan performance in section 5. Finally the contribution is summarized in section 6.

Post-print version of the article: R. Schroedter, M. Schwarzenberg, A. Dreyhaupt, R. Barth, T. Sandner, K. Janschek, "Microcontroller based closed-loop control of a 2D quasi-static/resonant microscanner with on-chip piezo-resistive sensor feedback", *Proc. of SPIE, MOEMS and Miniaturized Systems XVI*, vol. 10116, p. 1011605, 2017. DOI: 10.1117/12.2251802

For further information contact: schroedter@acin.tuwien.ac.at, https://orcid.org/0000-0003-3259-4571

2. 2D QUASI-STATIC/RESONANT MICRO SCANNER

The class of MSM structures presented below typically feature two electrostatically driven torsion axes of the gimbal-mounted mirror plate as shown in the layout Fig. 2. There, the inner resonant axis is operated in resonant mode with *in-plane* vertical comb drives providing near sinusoidal oscillations close to the mechanical resonance [6]. The outer quasi-static axis can distribute the resonant scan lines in a sawtooth, linear or even arbitrary manner among the projection area as shown in Fig. 1b. This staggered *out-of-plane* vertical comb drive is realized with an adhesive bonding process developed at IPMS [7,8] using a solid body mechanism that lowers the comb structure of about once the substrate height by indenters of the top wafer. The design process comprises finite element analyses as well as analytical calculations based on reduced order models to precisely predict mechanical and electrical properties, cf. [9]. Both gimballed axis are driven independently. To realize close-loop control of the mirror motion the MSM is equipped with piezo-resistive deflection sensors sensitive to changes of the mechanical stress close to the torsion springs. The piezo-resistive deflection sensors are realized as either thin isolated surface layers of polycrystalline silicon or the highly doped surface of the single crystalline device itself [3,10]. Four single piezo-resistive elements at each torsion axis are connected to a Wheatstone bridge circuit, providing a very sensitive and vastly temperature-independent deflection sensor.

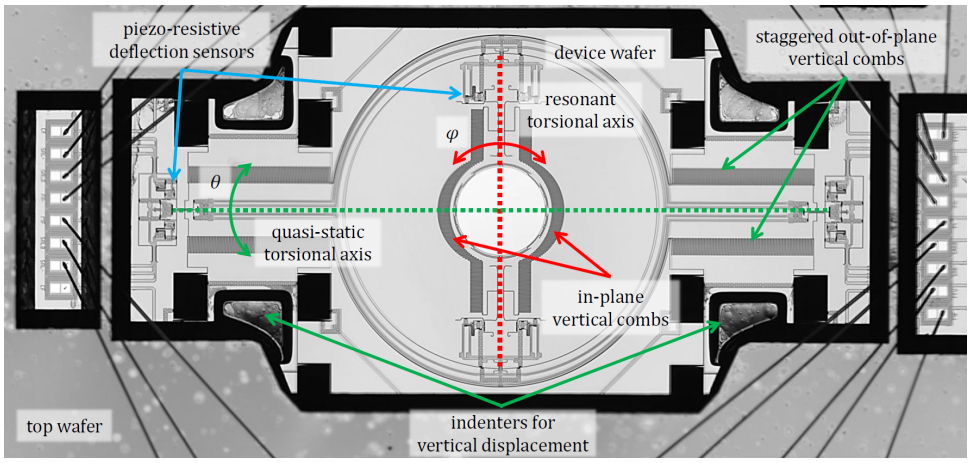

Figure 2: Layout of a typical 2D quasi-static/resonant microscanner from FhG-IPMS (see Fig. 1a), similar to the scanner used for the experiments below

Parameter identification for quasi-static axis Due to very low production tolerances the torque inertia can be determined sufficiently accurate with an finite element model in ANSYS resulting at $J = 2.5977\,\mathrm{kg}\,\mu\mathrm{m}^2$. The modal analysis gives the eigenfrequency $f_{0,\mathrm{sim}} = 175\,\mathrm{Hz}$ for the referring mirror. For identifying the real mirror eigenfrequency f_0 for small deflection and damping δ, we apply a voltage impulse of 10 V for 10 ms and evaluate the decaying curve shown in Fig. 3b. We determined the eigenfrequency $f_0 = 182.08\,\mathrm{Hz}$ and the damping $\delta = 3.67\,\mathrm{s}^{-1}$. The spring stiffness $k(\theta)$ is progressively raising with the deflection angle, because of the rectangular spring profile [2] and thus has a quadratic characteristic as described with Eq. (1).

$$k(\theta) = k_0 + k_2\theta^2 \tag{1}$$

We calculate the linear stiffness with $k_0 = J \cdot 2\pi f_0 = 3.4\,\mu\mathrm{Nm/rad}$. The quadratic stiffness $k_2 = 12.62\,\mu\mathrm{Nm/rad}^2$ is derived from the finite element model in ANSYS.

Post-print version of the article: R. Schroedter, M. Schwarzenberg, A. Dreyhaupt, R. Barth, T. Sandner, K. Janschek, "Microcontroller based closed-loop control of a 2D quasi-static/resonant microscanner with on-chip piezo-resistive sensor feedback", *Proc. of SPIE, MOEMS and Miniaturized Systems XVI*, vol. 10116, p. 1011605, 2017. DOI: 10.1117/12.2251802

For further information contact: schroedter@acin.tuwien.ac.at, https://orcid.org/0000-0003-3259-4571

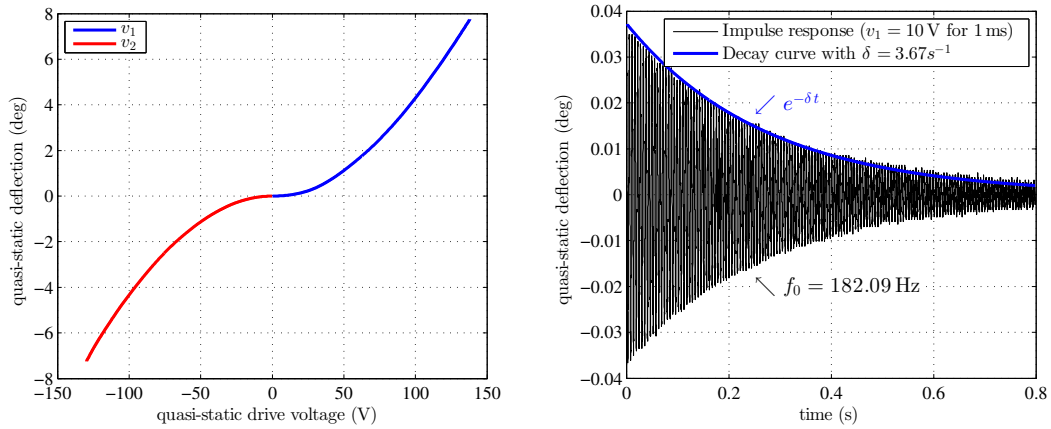

(a) Static deflection curve

(b) Decaying impulse response

Figure 3: Measurements for parameter identification of quasi-static axis: (a) static deflection curve, (b) impulse response

Parameter identification for resonant axis The resonant axis is driven in parametric resonance by applying a square-wave voltage with the frequency $f_{\text{res,drive}}$ and the amplitude v_{res}. This MEMS driving mode is realized with the drive frequency $f_{\text{res,drive}}$ being approximately the double of the mechanical oscillation frequency f_{res} of the resonant axis according Eq. (2).

$$f_{\text{res}} = \frac{1}{2} f_{\text{res,drive}} \tag{2}$$

This means that the electrostatic torque between the overlapping comb fingers accelerates the mirror mass in direction of zero deflection and the drive voltage is always switched off at zero deflection as illustrated in Fig. 4a. We identify the frequency-deflection family of curves for different drive voltages given with Fig. 4b. The frequency sweep is realized from higher frequencies down to the resonant frequency, where the oscillation stops abruptly because the mirror is pulled back to zero deflection instead of allowing a free oscillation. This effect is due to the *in-plane* comb drive principle: the driving torque is coupled into the system when the combs are *in-plane* and there is a relevant capacitance derivative $C'(\varphi)$ [11].

3. MODELING AND CONTROL METHOD

The gimbal-mounted axis of the microscanner are modeled as to individual low-damped spring-mass oscillators. By reason of the fundamental different operation modes, parametric resonance and quasi-static, we developed the two following control methods.

Closed-loop control of the quasi-static axis In [2] we have presented a flatness-based closed-loop control for the quasi-static axis of the micro scanning mirror. Using the principle of exact linearization for the nonlinear system this method requires several calculations of nonlinear characteristic curves. We now present a novel controller structure for the micro scanning mirror systems, that uses an exact feedforward linearization and the PID-like PID$^{\text{k}}$-controller to stabilize the system along the desired trajectory [12]. With the benefit of less online processing calculations, this control and observer algorithm is much faster than the original flatness-based closed-loop control and thus appropriate for a microcontroller implementation.

Post-print version of the article: R. Schroedter, M. Schwarzenberg, A. Dreyhaupt, R. Barth, T. Sandner, K. Janschek, "Microcontroller based closed-loop control of a 2D quasi-static/resonant microscanner with on-chip piezo-resistive sensor feedback", *Proc. of SPIE, MOEMS and Miniaturized Systems XVI*, vol. 10116, p. 1011605, 2017. DOI: 10.1117/12.2251802

For further information contact: schroedter@acin.tuwien.ac.at, https://orcid.org/0000-0003-3259-4571

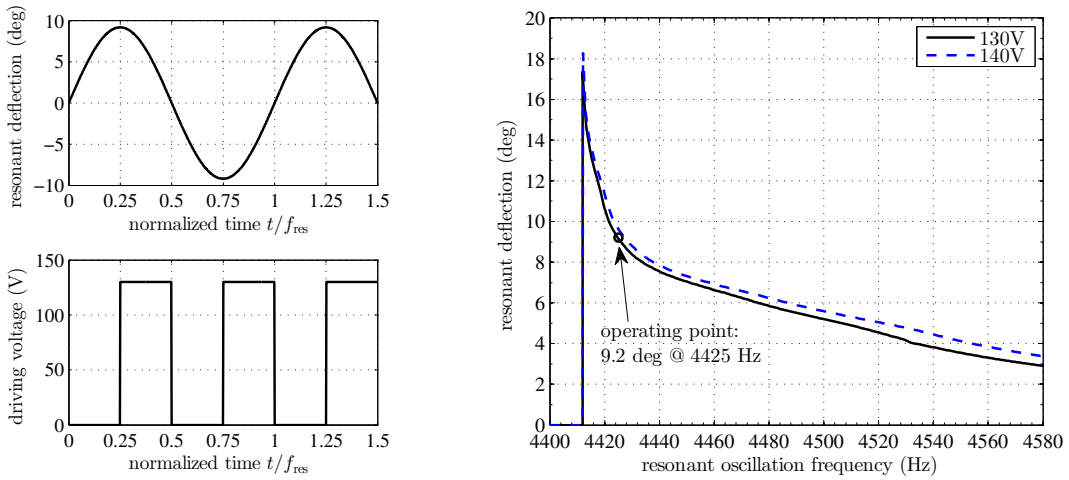

(a) resonant oscillation and driving voltage

(b) frequency-deflection curves

Figure 4: Resonant axis driving mode in parametric resonance: (a) driving scheme [11], (b) frequency-deflection curves

The nonlinear mechatronic model is given with Eq. (3), describing the mechanic part on the left side and the electrostatic drives for both combs on the right side.

$$J\ddot{\theta} + b\dot{\theta} + \tau_s(\theta) = \frac{1}{2}C_1'(\theta)v_1^2 + \frac{1}{2}C_2'(\theta)v_2^2, \tag{3}$$

Using the relations Eq. (4) we calculate the damping coefficient b, the nonlinear stiffness torque $\tau_s(\theta)$ and capacitance derivatives, which is determined from the static deflection curve (cf. Fig. 3a) as described in [2].

$$b = 2\delta J, \qquad \tau_s(\theta) = \int_0^\theta k(\bar{\theta})\,\mathrm{d}\bar{\theta} = k_0\theta + \frac{k_2}{3}\theta^3, \qquad C_i'(\theta) = \frac{2\tau_s(\theta)}{v_i^2(\theta)} \quad \text{for} \quad i = 1,2 \tag{4}$$

First, the system Eq. (3) is transformed into the state space representation Eq. (5) using the state $\boldsymbol{x} := (x_1, x_2) = (\theta, \dot{\theta})$ and the output $y := x_1 = \theta$ [2].

$$\dot{x}_1 = x_2, \qquad \dot{x}_2 = -\frac{b}{J}x_2 - \frac{\tau_s(x_1)}{J} + \underbrace{\frac{1}{2J}C_1'(\theta)v_1^2 + \frac{1}{2J}C_2'(\theta)v_2^2}_{u} \tag{5}$$

Based on the state space model Eq. (5) we realize the exact linearization using the new input $u^* \equiv u$ with Eq. (6).

$$u^* = u_\mathrm{d} + \ddot{\theta}_\mathrm{d} + \Lambda(e, \dot{e}) \quad \text{with} \quad u_\mathrm{d} = \frac{b}{J}\dot{\theta}_\mathrm{d} + \frac{\tau_s(\theta_\mathrm{d})}{J} \tag{6}$$

The control function $\Lambda(e, \dot{e})$ can be any controller stabilizing the error e and the velocity error $\dot{e}$. The feedforward linearization is described with u_d and $\ddot{\theta}_\mathrm{d}$. The control errors are defined with Eq. (7), where θ_d is the desired deflection angle and θ is the actual deflection angle.

$$e = \theta_\mathrm{d} - \hat{\theta}, \qquad \dot{e} = \dot{\theta}_\mathrm{d} - \dot{\hat{\theta}} \tag{7}$$

Post-print version of the article: R. Schroedter, M. Schwarzenberg, A. Dreyhaupt, R. Barth, T. Sandner, K. Janschek, "Microcontroller based closed-loop control of a 2D quasi-static/resonant microscanner with on-chip piezo-resistive sensor feedback", *Proc. of SPIE, MOEMS and Miniaturized Systems XVI*, vol. 10116, p. 1011605, 2017. DOI: 10.1117/12.2251802

For further information contact: schroedter@acin.tuwien.ac.at, https://orcid.org/0000-0003-3259-4571

For enabling the correct torque direction the drive voltages are charged according the sign of u^* with the switching relation Eq. (8).

$$v_1 = \begin{cases} \sqrt{\dfrac{2J}{C_1'(\theta_\mathrm{d})}u^*} & \text{for} \quad u^* > 0 \\ 0 & \text{for} \quad u^* \leq 0 \end{cases}, \qquad v_2 = \begin{cases} 0 & \text{for} \quad u^* > 0 \\ \sqrt{\dfrac{2J}{C_2'(\theta_\mathrm{d})}u^*} & \text{for} \quad u^* \leq 0 \end{cases} \tag{8}$$

We apply the PID$^\mathrm{k}$-controller $\Lambda(e, \dot{e})$ (Eq. (9)), which has a similar structure to the PID controller known from linear control theory [13].

$$\Lambda(e, \dot{e}) = k_\mathrm{P} e + k_\mathrm{I} \int e(t)\mathrm{d}t + k_\mathrm{D} \dot{e} \quad \text{with} \quad e = \theta_\mathrm{d} - \hat{\theta}, \dot{e} = \dot{\theta}_\mathrm{d} - \dot{\hat{\theta}} \tag{9}$$

The used piezo-resistive sensor feedback does only provide the actual deflection angle $\tilde{\theta}$, but not its derivative $\dot{\tilde{\theta}}$. For deriving the mirror's velocity we design an observer with an similar structure to the High-Gain observer from [2]. Nevertheless the reduced observer Eq. (10) has very simple structure, since the nonlinear characteristic curves $C_i'(\theta_\mathrm{d})$ and $\tau_\mathrm{s}(\theta_\mathrm{d})$ are precalculated with the desired deflection angle θ_d, and thus can be replaced with $\ddot{\theta}_\mathrm{d} + \Lambda(e, \dot{e})$ directly.

$$\dot{\hat{\theta}} = \int \left(\ddot{\theta}_\mathrm{d} + \Lambda(e, \dot{e}) + l_2 \left(\hat{\theta} - \tilde{\theta} \right) \right) \mathrm{d}t \tag{10a}$$

$$\hat{\theta} = \int \left(\dot{\hat{\theta}} + l_1 \left(\hat{\theta} - \tilde{\theta} \right) \right) \mathrm{d}t \tag{10b}$$

The observer gain $\boldsymbol{l} = (l_1, l_2)$ is placed with the Ackerman formula as described in [2]. The final control structure for the quasi-static axis is shown in Fig. 5. Here real-time calculation realizes the calculations for the reduced observer block Eq. (10), the error Eq. (7), the controller Eq. (9) and the reduced exact linearization Eq. (8).

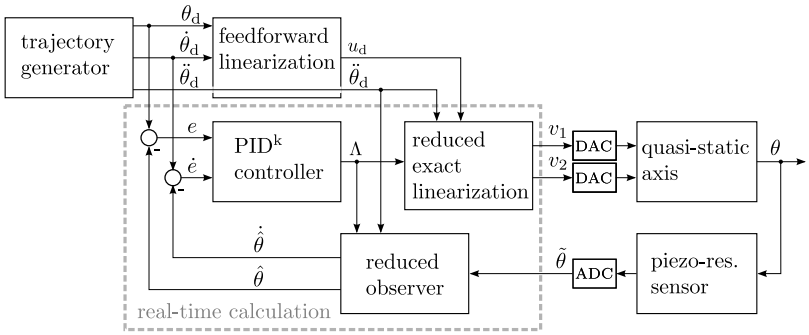

Figure 5: Closed-loop control of quasi-static axis

We apply a 8.85 Hz sawtooth trajectory for the quasi-static axis with the amplitude of ±7 deg as shown in Fig. 9. The jerk-limited trajectory design with a 3$^\mathrm{rd}$ order polynomial (cf. [1]) results in a ratio between the linear time and the refresh time of $\kappa_\mathrm{lin} = 91\,\%$. Assuming zero errors, we get the corresponding open-loop drive voltages and currents with Eq. (6) and Eq. (8) shown in Fig. 6.

Closed-loop control of scan amplitude of the resonant axis The resonant axis of the microscanner is a very low damped mechanical oscillator. Therefore applying a high voltage square wave signal the mirror is driven in parametric resonance oscillating sinusoidal according Eq. (11). The mechanical oscillation frequency f_res is exactly defined by the electrical driving frequency $f_\mathrm{res,drive}$ according to Eq. 2.

$$\varphi(t) \approx \hat{\varphi} \cdot \sin\left(2\pi f_\mathrm{res} \cdot t\right) \tag{11}$$

Post-print version of the article: R. Schroedter, M. Schwarzenberg, A. Dreyhaupt, R. Barth, T. Sandner, K. Janschek, "Microcontroller based closed-loop control of a 2D quasi-static/resonant microscanner with on-chip piezo-resistive sensor feedback", *Proc. of SPIE, MOEMS and Miniaturized Systems XVI*, vol. 10116, p. 1011605, 2017. DOI: 10.1117/12.2251802

For further information contact: schroedter@acin.tuwien.ac.at, https://orcid.org/0000-0003-3259-4571

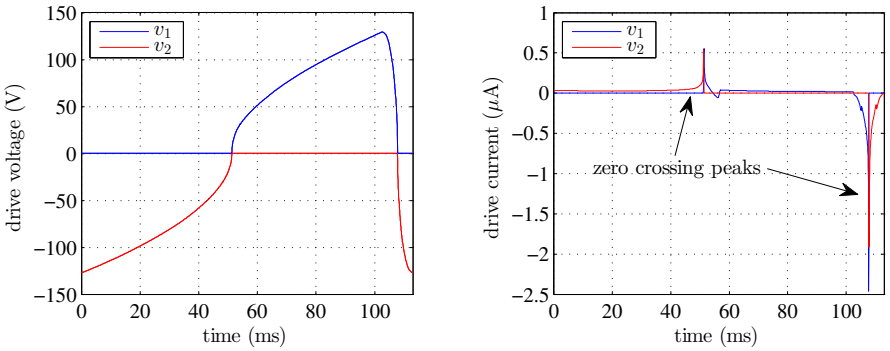

(a) Sawtooth drive voltage (b) Sawtooth drive current

Figure 6: Quasi-static drive voltages (a) and drive current (b) for the desired sawtooth trajectory, cf. Fig. 9

The amplitude v_{res} of electrical the driving signal affects directly the amplitude $\hat{\varphi}$ of the mechanical oscillation. Changing environmental condition, like temperature and pressure, can slightly affect the scan amplitude and therefore lead to blurred scan results. Therefore we stabilize the scan amplitude $\hat{\varphi}$ of the resonant axis in a closed-loop control as shown in Fig. 7. The piezo-resistive position sensor is fed back to a lock-in amplifier tuned to the mechanical frequency f_{res}. This narrow band filter is essential to get an applicable sensor feedback, since the low voltage signal is highly disturbed by the induced displacement charge from the high voltage drive signal, cf. Fig. 6b. The number N of mechanical oscillation periods used by the digital lock-in amplifier as well as the sampling frequency $f_{\mathrm{s}} = 1/T_{\mathrm{s}}$ are the tuning parameters for this filter considering $T_{\mathrm{s}} > N/f_{\mathrm{res}}$. We stabilize the amplitude error $\epsilon = \hat{\varphi}_{\mathrm{d}} - \hat{\varphi}$ between desired amplitude $\hat{\varphi}_{\mathrm{d}}$ and the lock-in amplifier output $\hat{\varphi}$ with the time-discrete PID controller Eq. (12) and its control coefficients $K_{\mathrm{P}}, K_{\mathrm{I}}, K_{\mathrm{D}}$.

$$C(z) = K_{\mathrm{P}} + K_{\mathrm{I}}\frac{z}{z-1} + K_{\mathrm{D}}\frac{z-1}{z} \tag{12}$$

The controller output is converted into an analog signal and acts as the control voltage for the amplitude of the electrical driving signal $\hat{v}_{\mathrm{res}}$. Note that implementing the square wave switching at the high voltage significantly reduces the bandwidth of the high voltage amplifier. The oscillation phase can be determined with the lock-in amplifier by comparing the start of the analog to digital conversion and the reference signal at f_{res}. By shifting the phase it is possible to correct timing of oscillation and to synchronize with other microscanners.

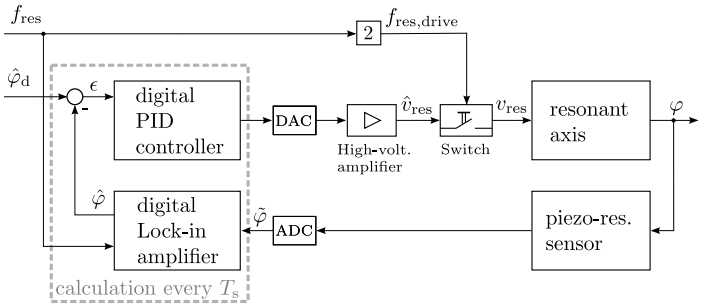

Figure 7: Closed loop control for resonant axis

Post-print version of the article: R. Schroedter, M. Schwarzenberg, A. Dreyhaupt, R. Barth, T. Sandner, K. Janschek, "Microcontroller based closed-loop control of a 2D quasi-static/resonant microscanner with on-chip piezo-resistive sensor feedback", *Proc. of SPIE, MOEMS and Miniaturized Systems XVI*, vol. 10116, p. 1011605, 2017. DOI: 10.1117/12.2251802

For further information contact: schroedter@acin.tuwien.ac.at, https://orcid.org/0000-0003-3259-4571

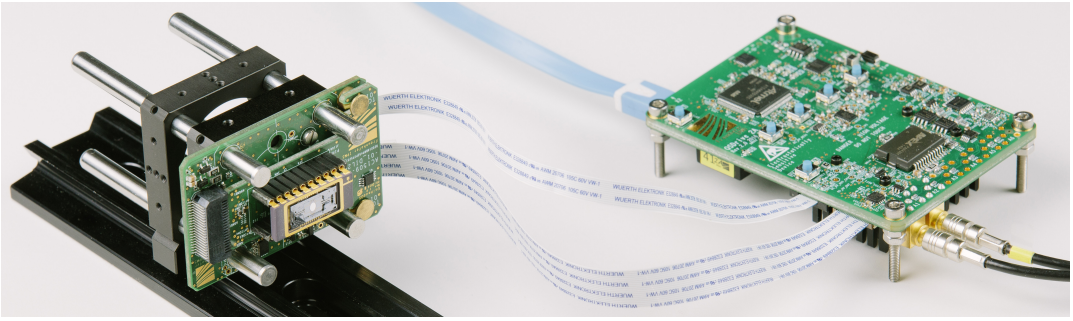

Figure 8: Microscanner mounted on head electronic and connected with microcontroller board

4. MICROCONTROLLER-BASED DRIVER

We developed a microcontroller-based driver for real-time control of the microscanner shown in Fig. 8. The microscanner is mounted on a scan head board (60 mm × 40 mm size), where an 8^{th}-order Bessel filter circuit and the analog-digital converter for processing the piezo-resistive sensor signal is located. As presented in [1], electromagnetic coupling from the drive high-voltage signals does heavily disturb the low voltage sensor signal. Nevertheless this novel direct mounting allows very short wires and together with analog Bessel filtering and the analog-digital conversion we do now provide an adequate sensor quality suitable as position feedback. Furthermore the switching circuit for high voltage square wave generation used for driving the resonant axis is located on the scan head board to reduce the electromagnetic emission. The scan head is remoted via flexible flat cables by a microcontroller board allowing an easy integration in customized applications. The microcontroller (85 mm × 60 mm size) board consists of an ARM-Cortex controller for data processing, a complex programmable logic device (CPLD) and a clock controlling unit enabling closed-loop control frequencies up to 50kHz. A two-channel high-voltage driving unit for the quasi-static mirror axis generates arbitrary dynamic driving signals of up to 200 V with a slew-rate of 9 V/μs having a precision error of less than $\pm 0,5\%$ on a jump from zero volt to 200 V. The signal quality is determined by the standard deviation of 50 mV. Regarding the voltage curve in Fig. 6a, there is a very high voltage change needed at the zero deflection crossings due to the quadratic relation Eq. (8) resulting in displacement current peaks shown in Fig. 6b. The power consumption while running is less than 5.4 W. Multiple interfaces serve as user-communication and for synchronization of the driving regime of each mirror axis.

5. PERFORMANCE EVALUATION

With the frequency ratio of 500 between the resonant axis at $f_{\text{res}} = 4425$ Hz and the quasi-static axis at $f_{\text{qs}} = 8.85$ Hz, the Lissajous scan pattern of in total 1000 lines is repeated every 113 ms with 910 lines in the linear scan time and 90 lines during the refresh time of the quasi-static sawtooth trajectory according Eq. (13). Assuming a quadratic pixel raster met by the scan pattern, it resolves 1208 pixel on the resonant axis. Nevertheless the estimation Eq. (13) supposes no gap between the scan lines for high deflections of the resonant axis due to its sinusoidal scan form.

$$N_{\text{quasi-st./res.}} = 2\frac{f_{\text{res}}}{f_{\text{qs}}} \cdot \kappa_{\text{lin}} = 910 \tag{13}$$

We measured the scan result using an experimental setup with a laser beam deflection on a position sensitive device (PSD) as introduced in [1]. Fig. 9 shows the measured control results of the quasi-static axis in open-loop and closed-loop control. In open-loop control the quasi-static axis follows the sawtooth trajectory with a substantial residual oscillation at its eigenfrequency $f_0 = 182.09$ Hz of about $\pm 2\,\%$ error. During the linear scan phase the error is slightly decreasing, representing the very low damping δ. The peak at the zero deflection

Post-print version of the article: R. Schroedter, M. Schwarzenberg, A. Dreyhaupt, R. Barth, T. Sandner, K. Janschek, "Microcontroller based closed-loop control of a 2D quasi-static/resonant microscanner with on-chip piezo-resistive sensor feedback", *Proc. of SPIE, MOEMS and Miniaturized Systems XVI*, vol. 10116, p. 1011605, 2017. DOI: 10.1117/12.2251802

For further information contact: schroedter@acin.tuwien.ac.at, https://orcid.org/0000-0003-3259-4571

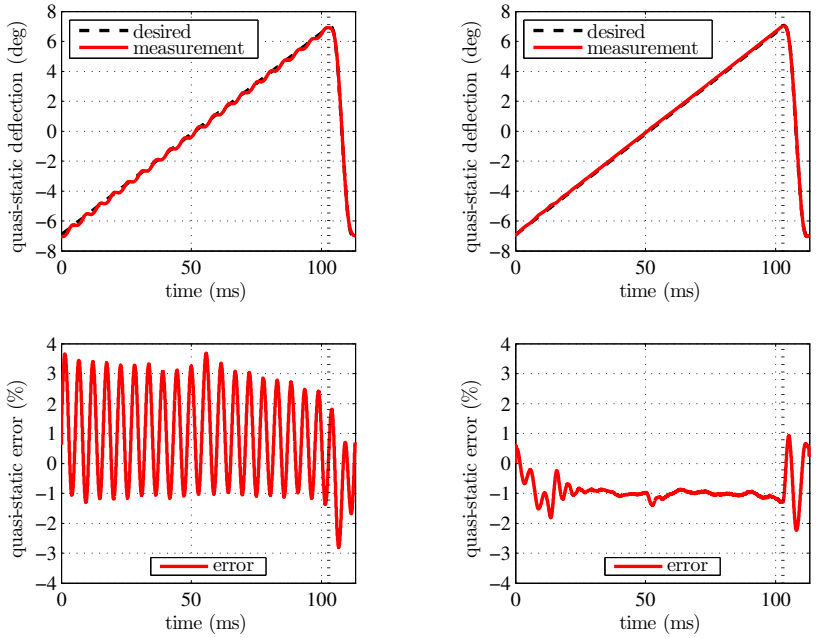

(a) Open-loop (b) Closed-loop

Figure 9: Quasi-static scan trajectory and error in (a) open-loop and (b) closed-loop

crossing is due to the high displacement current, cf. Fig. 6b, required to change the deflection side, but damped by imperfect electrical circuit or a substantial equivalent serial impedance.
The closed-loop control does remarkably damp this parasitic oscillation to lower than ±0.2 % after a transient oscillation of about 20 ms. This transient oscillation is caused by the feature of disabling the control during the refresh time, which leads to in total better control results. Again a small increase of error can be detected at the zero crossing. Regarding the sensor result for one period and its Fourier transformation shown in Fig. 10, we recognize major error components for the parasitic *in-plane* mode at $f_{\mathrm{par}} = 2125\,\mathrm{Hz}$, the frequency f_{res} of the resonant axis and its half. Since the experiments are performed in laboratory conditions with stable temperature, the sensor signal did not show a temperature drift. Nevertheless a temperature compensation in application conditions can be realized by measuring the piezo-resistive sensor resistances and deposing temperature reference curves.

Fig. 11 shows the 2D scan pattern within the linear area or service time of the quasi-static axis, this means the laser was deactivated during the refresh time. Fig. 11a and Fig. 11b demonstrate the measurement results detected on a PSD. Fig. 11c and Fig. 11d are showing the same projection on a screen with a laser projecting on the microscanner through a hole in the middle of the screen. Comparing the results of Fig. 11a and Fig. 11c with Fig. 9a, the residual oscillation of the quasi-static axis with its eigenfrequency f_0 can be identified. With closing the loop this error is significantly reduced and a high uniformity of the pixel density is achieved as shown in Fig. 11b, Fig. 11d and Fig. 9b.

Post-print version of the article: R. Schroedter, M. Schwarzenberg, A. Dreyhaupt, R. Barth, T. Sandner, K. Janschek, "Microcontroller based closed-loop control of a 2D quasi-static/resonant microscanner with on-chip piezo-resistive sensor feedback", *Proc. of SPIE, MOEMS and Miniaturized Systems XVI*, vol. 10116, p. 1011605, 2017. DOI: 10.1117/12.2251802

For further information contact: schroedter@acin.tuwien.ac.at, https://orcid.org/0000-0003-3259-4571

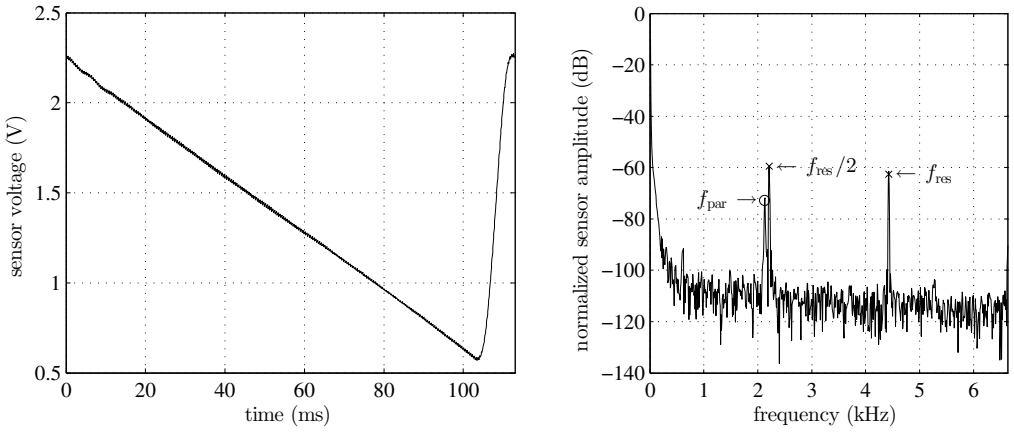

(a) Quasi-static sensor signal (b) FFT

Figure 10: Piezo-resistive sensor signal of quasi-static axis (a) and its Fourier transform (b)

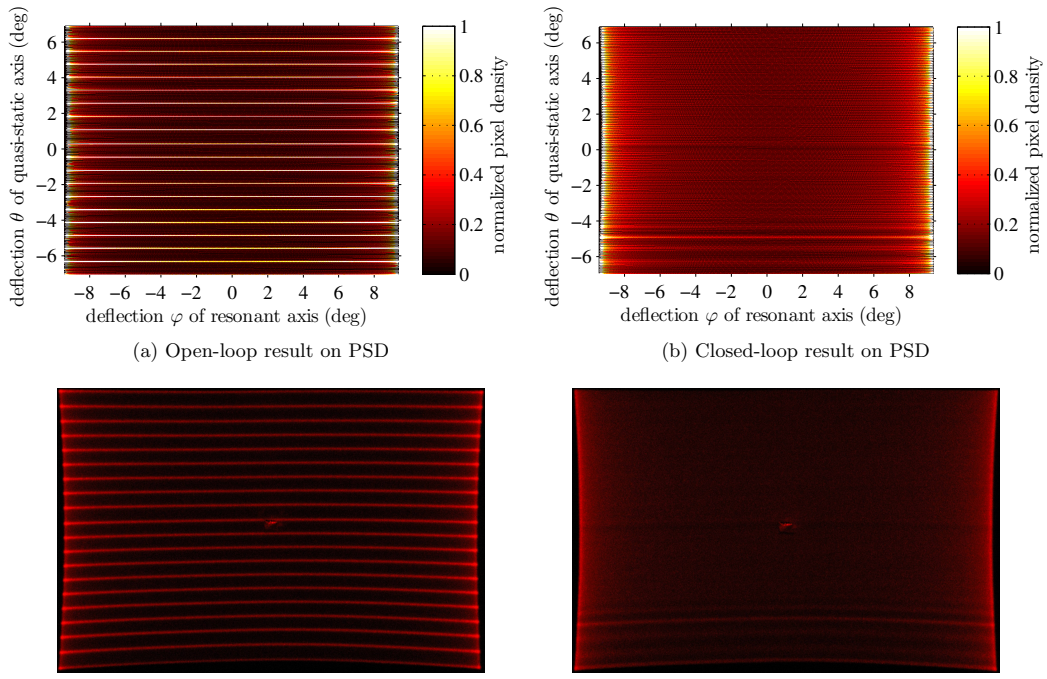

(a) Open-loop result on PSD (b) Closed-loop result on PSD

(c) Open-loop result on screen (d) Closed-loop result on screen

Figure 11: 2D scan pattern in open-loop (a), (c) and closed-loop (b), (d); measured with PSD (a),(b); photograph of screen (c),(d)

Post-print version of the article: R. Schroedter, M. Schwarzenberg, A. Dreyhaupt, R. Barth, T. Sandner, K. Janschek, "Microcontroller based closed-loop control of a 2D quasi-static/resonant microscanner with on-chip piezo-resistive sensor feedback", *Proc. of SPIE, MOEMS and Miniaturized Systems XVI*, vol. 10116, p. 1011605, 2017. DOI: 10.1117/12.2251802

For further information contact: schroedter@acin.tuwien.ac.at, https://orcid.org/0000-0003-3259-4571

6. SUMMARY

We demonstrated a quasi-static/resonant micro scanning mirror with *in-plane* and *out-of-plane* staggered vertical comb drive performing a 2D raster scan with about 1208×910 pixels comparable to XGA+ resolution and a refresh rate of 8.85 Hz. With the developed small size microcontroller setup, realizing the command drive voltages together with the real-time closed-loop control, we eliminated residual oscillations for desired sawtooth motion profiles of the quasi-static axis. Based on polycrystalline silicon technology the on-chip piezo-resistive deflection sensors provide suitable signal quality to serve as feedback signal, enhanced by analog and digital filters. In closed-loop operation the linearity of scan trajectory is significantly improved compared to open-loop control resulting in errors less than $\pm 1\,\%$ in the linear scan area.

REFERENCES

[1] Schroedter, R., Janschek, K., and Sandner, T., "Jerk and Current Limited Flatness-based Open Loop Control of Foveation Scanning Electrostatic Micromirrors," in [*International Federation of Automation and Control (IFAC) Conference*], 2685–2690 (2014).

[2] Schroedter, R., Sandner, T., Janschek, K., Roth, M., and Hruschka, C., "Real-time closed-loop control for micro mirrors with quasistatic comb drives," in [*MOEMS and Miniaturized Systems XV*], *Proc. SPIE* **9760**, 976009–976009–13 (2016).

[3] Grahmann, J., Dreyhaupt, A., Drabe, C., Schroedter, R., Kamenz, J., and Sandner, T., "MEMS-mirror based trajectory resolution and precision enabled by two different piezoresistive sensor technologies," in [*MOEMS and Miniaturized Systems XV*], *Proc. SPIE* **9760**, 976006–976006–11 (2016).

[4] Holmström, S. T. S., Baran, U., and Urey, H., "MEMS Laser Scanners: A Review," *Journal of Microelectromechanical Systems* **23**(2), 259–275 (2014).

[5] Drabe, C., Kallweit, D., Dreyhaupt, A., Grahmann, J., Schenk, H., and Davis, W., "Bi-resonant scanning mirror with piezoresistive position sensor for wvga laser projection systems," in [*MOEMS and Miniaturized Systems XI*], *Proc. SPIE* **8252**, 825209–825209–10 (2012).

[6] Schenk, H., Sandner, T., Drabe, C., Klose, T., and Conrad, H., "Single crystal silicon micro mirrors," *physica status solidi* **6**(3), 728–735 (2009).

[7] Jung, D., Sandner, T., Kallweit, D., and Schenk, H., "Vertical comb drive microscanners for beam steering, linear scanning, and laser projection applications," in [*MOEMS and Miniaturized Systems XI*], *Proc. SPIE* **8252**, 82520U–82520U–10 (2012).

[8] Sandner, T., Grasshoff, T., Schwarzenberg, M., Schroedter, R., and Schenk, H., "Quasistatic microscanner with linearized scanning for an adaptive three-dimensional laser camera," *Journal of Micro/Nanolithography, MEMS, and MOEMS* **13**(1), 011114 (2014).

[9] Sandner, T., Grasshoff, T., Wildenhain, M., and Schenk, H., "Synchronized microscanner array for large aperture receiver optics of LIDAR systems," in [*MOEMS and Miniaturized Systems IX*], *Proc. SPIE* **7594**, 75940C–75940C–12 (2010).

[10] Sandner, T., Conrad, H., Klose, T., and Schenk, H., "Integrated Piezo-resistive Position sensor for Microscanning Mirrors," in [*IEEE/LEOS International Conference on Optical MEMS and Nanophotonics*], 195–196 (2007).

[11] Schenk, H., Durr, P., Haase, T., Kunze, D., Sobe, U., Lakner, H., and Kuck, H., "Large deflection micromechanical scanning mirrors for linear scans and pattern generation," *IEEE Journal of Selected Topics in Quantum Electronics* **6**(5), 715–722 (2000).

[12] Hagenmeyer, V. and Delaleau, E., "Exact feedforward linearization based on differential flatness," *International Journal of Control* **76**(6), 537–556 (2003).

[13] Janschek, K., [*Mechatronic Systems Design - Methods, Models, Concepts*], Springer (2012).

Post-print version of the article: R. Schroedter, M. Schwarzenberg, A. Dreyhaupt, R. Barth, T. Sandner, K. Janschek, "Microcontroller based closed-loop control of a 2D quasi-static/resonant microscanner with on-chip piezo-resistive sensor feedback", *Proc. of SPIE, MOEMS and Miniaturized Systems XVI*, vol. 10116, p. 1011605, 2017. DOI: 10.1117/12.2251802

For further information contact: schroedter@acin.tuwien.ac.at, https://orcid.org/0000-0003-3259-4571